the methyl groups establishes facile rotation about the Zr–Os line (the process maintains the integrity of each trans H–Os–P vector).

The presence of low-energy stretching frequencies (e.g., 1710 and 1565 cm^{-1} in **4b**) suggests hydride bridges are also present in compounds **4**.

The wide variety of M–H, M′–H, and M–H–M′ bonds present in **3** and **4**, as well as the potential for creating unsaturation by H_2 or CH_4 elimination from **3b**, **4b**, and **4c**, motivate our current reactivity studies.

Acknowledgment. We thank NSF (CHE-8305281) for financial support, and Johnson, Matthey Co. for the loan of chemicals. We thank Scott Horn for skilled technical assistance.

Supplementary Material Available: Listing of atom coordinates, bond lengths, and bond angles for $Cp_2ZrClH_3Os(PMe_2Ph)_3$ (6 pages). Ordering information is given on any current masthead page.

Iron(III)-Catalyzed Oxygenation of Catechols. Structure of (Nitrilotriacetato)(3,5-di-*tert*-butylcatecholato)-ferrate(III) Dianion

L. S. White, P. V. Nilsson, L. H. Pignolet, and L. Que, Jr.*

Department of Chemistry, University of Minnesota Minneapolis, Minnesota 55455

Received September 17, 1984

A variety of metal complexes have been reported that effect the oxidative cleavage of catechols.[1-7] These systems serve as models for the reactions catalyzed by catechol 1,2-dioxygenase and protocatechuate 3,4-dioxygenase, enzymes in which the proposed mechanism of oxygen incorporation involves substrate activation by the active site ferric center.[8] One system of particular interest is that reported by Weller and Weser,[7] consisting of the Fe(III)–nitrilotriacetate complex in an organic solvent–borate buffer mixture, the only Fe(III) system thus far that shows catechol cleavage activity. Over a period of days and in the presence of oxygen, 3,5-di-*tert*-butylcatechol is catalytically converted to 3,5-di-*tert*-butyl-5-(carboxymethyl)-2-furanone in 80% yield, the highest reported for any model system to date.

Under the appropriate conditions, salts of $[Fe(NTA)DBC]^{2-}$[9] can be isolated with a stoichiometry that suggests that the catecholate ligand is chelated to the iron. This complex reacts with oxygen in DMF over 4 days to yield cleavage product in 80% yield. The reactivity of this complex contrasts that of a related system, $[Fe(salen)DBC]^-$, which is reported to be unreactive toward dioxygen.[10] The lack of reactivity of $[Fe(salen)DBC]^-$ has been suggested to arise from the stability of the chelated structure. The $E^{\circ\prime}$ for the DBSQ/DBC couple was found to be -423 mV vs. SCE in the complex as compared to -1340 mV in the free ligand,[11] a stabilization of the catecholate oxidation state by nearly a volt. Electrochemical studies of $[Fe(NTA)DBC]^{2-}$ show even greater stabilization for the DBSQ/DBC couple in this complex; $E^{\circ\prime}$ is found to be -268 mV vs. SCE in DMF. Thus electron transfer from both chelated catecholate complexes to dioxygen is thermodynamically unfavorable. However, it is clear that $[Fe(NTA)DBC]^{2-}$ reacts with dioxygen.

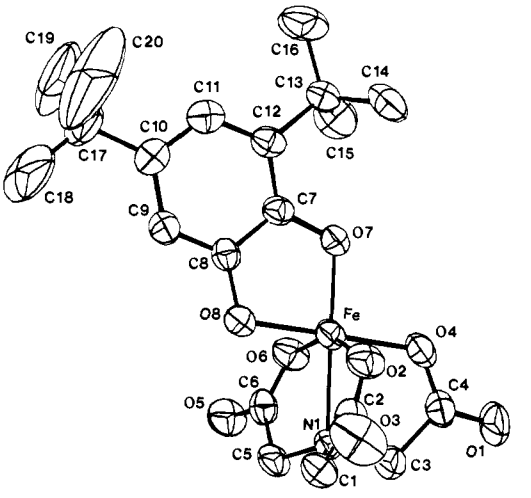

Figure 1. Structure of $[Fe(NTA)DBC]^{2-}$ showing 50% probability thermal ellipsoids and atom labeling scheme. Hydrogen atoms omitted for clarity. Selected bond distances in Å: Fe–N1, 2.224 (3); Fe–O2, 2.034 (3); Fe–O4, 2.002 (3); Fe–O6, 2.039 (3); Fe–O7, 1.887 (3); Fe–O8, 1.979 (3).

The structure of the $[Fe(NTA)DBC]^{2-}$ complex suggests a possible explanation for its reactivity. Crystallographic quality crystals can be obtained from anaerobic DMF solutions containing stoichiometric amounts of Fe(NTA), $DBCH_2$, and dabco. $(dabcoH)_2[Fe(NTA)DBC]\cdot DMF$ crystallizes as hexagonal plates in the space group $P2_1/n$.[12] Refinement of the data yields an ORTEP plot of the anionic complex shown in Figure 1. The complex is a distorted octahedron featuring a tetradentate NTA and a bidentate catecholate. The most striking feature of this structure is the significant difference in the two Fe–O(DBC) bond lengths—1.887 (3) and 1.979 (3) Å. By comparison, the Fe–O(catechol) bonds in $[Fe(salen)cat]^-$ are both 1.99 Å long[13] and the Fe–O bonds in $[Fe(cat)]_3^{3-}$ show a range of 2.00–2.04 Å.[14] Steric effects are not responsible for the different bond lengths in $[Fe(NTA)DBC]^{2-}$; indeed, the DBC oxygen proximal to the 3-*tert*-butyl group, has the shorter Fe–O bond. Close examination of the structure reveals the source of this large difference: the shorter Fe–O bond is trans to the Fe–N bond. Due to the constraints on the NTA ligand required by its tetradentate ligation, the Fe–N bond is 2.224 (3) Å, which is longer than those in less constrained complexes such as $[Fe(acac)_2trien]^+$ (2.175 Å),[15]

(1) (a) Tsuji, J.; Takayanagi, H.; Sakai, I. *Tetrahedron Lett.* **1975**, 1245–1246. (b) Tsuji, J.; Takayanagi, H. *J. Am. Chem. Soc.* **1974**, *96*, 7349–7350.

(2) Brown, D. G.; Beckmann, L.; Ashby, C. H.; Vogel, G. C.; Reinprecht, J. T. *Tetrahedron Lett.* **1977**, 1363–1364.

(3) (a) Rogic, M. M.; Demmin, T. R. *J. Am. Chem. Soc.* **1978**, *100*, 5472–5487. (b) Rogic, M. M.; Demmin, T. R. *J. Org. Chem.* **1980**, *45*, 4210–4214. (c) Demmin, T. R.; Swerdloff, M. D.; Rogic, M. M. *J. Am. Chem. Soc.* **1981**, *103*, 5795–5804.

(4) Funabiki, T.; Sakamoto, H.; Yoshida, S.; Tamara, K. *J. Chem. Soc., Chem. Commun.* **1979**, 754–755.

(5) Matsumoto, M.; Kuroda, K. *J. Am. Chem. Soc.* **1982**, *104*, 1433–1434.

(6) Tatsuno, Y.; Tatsuda, M.; Otsuka, S. *J. Chem. Soc., Chem. Commun.* **1982**, 1100–1101.

(7) Weller, M. G.; Weser, V. *J. Am. Chem. Soc.* **1982**, *104*, 3752–3754.

(8) (a) Que, L., Jr. *Coord. Chem. Rev.* **1983**, *50*, 73–108. (b) Jefford, C. W.; Cadby, P. A. *Forstchr. Chem. Org. Naturst.* **1981**, *40*, 191–265.

(9) Abbreviations used: NTA, nitrilotriacetate; $DBCH_2$, 3,5-di-*tert*-butylcatechol; salen, *N,N′*-ethylenebis(salicylideneamine); DBSQ, 3,5-di-*tert*-butyl-*o*-benzosemiquinone anion; dabco, 1,4-diazabicyclo[2.2.2]octane; $catH_2$, catechol; Hacac, 2,4-pentanedione; trien, triethylenetetraamine; EHPG, *N,N′*-ethylenebis(*o*-hydroxyphenylglycine) tetraanion; tacn, 1,4,7-triazacyclononane; OAc, acetate; EDTA, ethylenediamine-*N,N,N′,N′*-tetraacetate; pip, piperidine.

(10) Lauffer, R. B.; Heistand, R. H., II; Que, L., Jr. *J. Am. Chem. Soc.* **1981**, *103*, 3947–3949.

(11) Nanni, E. J.; Stallings, M. D.; Sawyer, D. T. *J. Am. Chem. Soc.* **1980**, *102*, 4481–4485.

(12) $(dabcoH)_2[Fe(NTA)DBC]$ crystallizes in the monoclinic system, space group $P2_1/n$, with a = 17.874 (4) Å, b = 9.963 (3) Å, c = 23.117 (9) Å, β = 105.38 (3)°, V = 3969.3 Å^3, ρ_{obsd} = 1.28 g cm^{-3}, ρ_{calcd} = 1.278 g cm^{-3}, and Z = 4. With the use of 3413 unique observed reflections collected at 298 K with Mo K$\bar{\alpha}$ (λ = 0.7107 Å) radiation out to 2θ = 48° on an Enraf-Nonius CAD4 X-ray diffractometer, the structure was solved by Patterson and Fourier methods and refined anisotropically to a final value for the discrepancy index R_1 of 0.067. Atomic positional and thermal parameters are provided as supplementary material. Full details will be reported elsewhere.

(13) Lauffer, R. B.; Heistand, R. H., II; Que, L., Jr. *Inorg. Chem.* **1983**, *22*, 50–55.

(14) Raymond, K. N.; Isied, S. S.; Brown, L. D.; Fronczek, F. R.; Nibert, J. H. *J. Am. Chem. Soc.* **1976**, *98*, 1767–1774.

0002-7863/84/1506-8312$01.50/0 © 1984 American Chemical Society

$[Fe(EHPG)]^-$ (2.16 Å),[16] and $[Fe_2(tacn)_2(OAc)_2O]^{2+}$ (2.18 Å).[17] The Fe–N bond in $[Fe(EDTA)H_2O]^-$[18] is similarly constrained and exhibits a bond length of 2.33 Å. The weaker Fe–N bond results in the stronger Fe–O bond trans to it, giving rise to an unsymmetrically chelated catecholate. This may enhance the formation of the monodentate form derived from breaking the longer Fe–O bond. We propose that this monodentate form is the species that reacts with O_2 and that the reaction proceeds by the mechanism shown below.

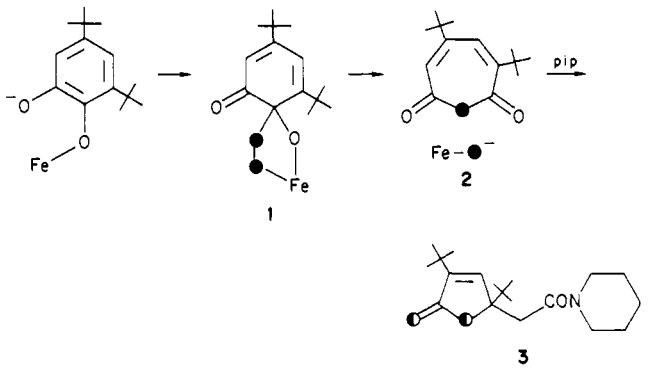

Studies on the reaction of $(pipH)_2[Fe(NTA)DBC]$ with $^{18}O_2$ in DMF provide further mechanistic insight. The product from the reaction, **3**,[19] obtained in 80% yield, shows the clean incorporation of one ^{18}O (98%) label. The CI-MS data on the product show the M + 1 ion at m/z 324 and the M + 1 − CH_4 ion at m/z 308, while the EI-MS data show a base peak at m/z 126 corresponding to the acetamide side chain, showing that the label is localized on the furanone ring. This is consistent with the formation of an intermediate anhydride, **2**, which is subsequently cleaved by piperidine. Attack of the anhydride at the C-6 carbonyl is expected on steric grounds.

This clean incorporation of a single ^{18}O label contrasts the results from other model cleavage reactions where substantial label scrambling occurs; the cleavage product in the latter cases exhibits varying amounts of label, ranging from molecules with no label incorporated to molecules with as many as four labels incorporated.[20] Such scrambling is thought to result from intermolecular side reactions involving the peroxy adduct **1**; these side reactions probably lower the effective yield of cleavage product as well. The absence of such scrambling in the Fe–NTA system and the high reaction yield suggest an additional role for the iron in the mechanism of oxidative cleavage. We propose that the ferric center coordinates the peroxy adduct and channels its decomposition toward the anhydride by stabilizing the oxide anion which would result from the Criegee rearrangement. This study thus suggests that the ferric center in the dioxygenases not only participates in the activation of substrate but also facilitates the latter stages of the reaction. In the enzyme active site, the oxide anion formed as a result of the rearrangement remains in the active site and acts as the nucleophile that opens the anhydride, thereby giving rise to dioxygenated product.

Acknowledgment. This work was supported by the National Institutes of Health (GM-33162). L.Q. is a Fellow of the Alfred P. Sloan Foundation (1982–1986) and the recipient of an NIH Research Career Development Award (AM 02136, 1982–1987).

Supplementary Material Available: Tables of atomic positional and thermal parameters for $(dabcoH)_2[Fe(NTA)DBC]\cdot DMF$ (5 pages). Ordering information is given on any current masthead page.

(15) Sinn, E.; Sim, G.; Dose, E. V.; Tweedle, M. F.; Wilson, L. J. *J. Am. Chem. Soc.* **1978**, *100*, 3375–3390.
(16) Bailey, N. A.; Cummins, D.; McKenzie, E. D.; Worthington, J. M. *Inorg. Chim Acta* **1981**, *50*, 111–120.
(17) Wieghardt, K.; Pohl, K.; Gebert, W. *Angew. Chem., Int. Ed. Engl.* **1983**, *22*, 727.
(18) Lind, M. D.; Hamor, M. J.; Hamor, T. A.; Hoard, J. L. *Inorg. Chem.* **1964**, *3*, 34–43.
(19) Characterization of unlabeled **3**: mp 116–117 °C; ^1H NMR δ 1.00 (s, 9 H), 1.22 (s, 9 H), 1.54 (m, 6 H), 2.90 and 3.07 (AB q, J_{AB} = 53 Hz, 2 H), 3.41 (m, 4 H), 7.14 (s, 1 H); CI-MS (CH_4), m/z 322 (M + 1), 306 (M + 1 − CH_4); EI-MS, m/z 321 (M), 306 (M − CH_3), 265, 250, 180, 153, 126 (M − $C_{12}H_{19}O_2$, loss of furanone).
(20) Label scrambling has been observed in $^{18}O_2$ experiments using systems discussed in ref 2, 4, 5, and 6. White, L. S.; Que, L., Jr., manuscript in preparation.

New Stereocontrolled Approach to 3-Deoxy-D-*manno*-2-octulosonic Acid Containing Disaccharides

Francoise Paquet and Pierre Sinaÿ*

Laboratoire de Biochimie Structurale, E.R.A. 739
U.E.R. de Sciences Fondamentales et Appliquées
45046 Orléans Cédex, France
Received July 30, 1984

3-Deoxy-D-*manno*-2-octulosonic acid (KDO) occurs as a ketosidic component in all lipopolysaccharides (LPS) and several acidic exopolysaccharides (K antigens) located at the cell surface of Gram-negative bacteria.[1] On the basis of ^{13}C and ^1H NMR results, it is believed that KDO displays in bacteria both the β- and α^2-D anomeric configurations. It is interesting to mention that sialic acid presents only one anomeric configuration[3] (α-D anomer).

The synthesis of KDO-containing oligosaccharides has only been approached so far by conventional glycosylation procedures[4] involving either methyl 3-deoxy-4,5,7,8-tetra-*O*-acetyl-α-D-*manno*-octulopyranosonate chloride or bromide. We would like to present a new and stereocontrolled approach to this synthetic challenge.

2,3-Di-*O*-benzyl-D-mannose[5] (**1**) was converted (EtSH, HCl, 24h, O °C) into **2** (85%) mp 78–79 °C (ether–hexane) then ((i) Ac_2O, pyridine, 12 h, room temperature; (ii) red HgO, $BF_3\cdot Et_2O$, aqueous THF, 40 min, room temperature) into the aldehyde **3** (93%), which represents the general precursor of the KDO unit.

Condensation of the aldehyde **3** with the phosphonate **4**[7] (THF, NaH, 1 h, 0 °C) afforded the *E* and *Z*[8] enol ethers **5** and **11** (85%, *E*/*Z* ratio 3:2), easily separated by silica gel chromatography. Deacetylation (MeONa–MeOH) gave the *E* and *Z* enol ethers **6** (95%) and **12** (95%). When the *E* isomer **6** was submitted to Hg(II)-induced cyclization [(i) $Hg(OCOCF_3)_2$, THF, 2 h, 0 °C; (ii) aqueous KCl, 12 h, 0 °C], the chloromercurio derivative **7**, mp 114–115 °C (ethanol), was obtained *as the only detectable isomer* in about 85%. The remarkable stereospecificity of the mercuriocyclization may be rationalized as previously postulated by us[7] in the case of sialic acid. The regiospecificity of the cyclization is also noteworthy. Demercuration of **7** (Ph_3SnH, AcONa, toluene, 3 h, room temperature) gave **8** (90%), which after catalytic hydrogenolysis (Pd/C) was converted into the anomerically pure β-linked disaccharide **9**[9,10] (90%) and finally

(1) Unger, F. M. *Adv. Carbohydr. Chem. Biochem.* **1981**, *38*, 323–388.
(2) Jennings, H. J.; Rosell, K.-G.; Johnson, K. G. *Carbohydr. Res.* **1982**, *105*, 45–56. Unger, F. M.; Christian, R.; Schultz, G.; Waldstätten, P.; Brade, H.; Zähringer, U.; Rietschel, E. Th. *Abstr. Pap.—Int. Carbohydr. Symp. 12th* **1984**, 348 and references therein.
(3) Schauer, R. "Sialic Acids, Chemistry, Metabolism, and Function"; Springer Verlag: New York, 1982.
(4) Waldstätten, P.; Christian, R.; Schultz, G.; Unger, F. M.; Kosma, P.; Kratky, C.; Paulsen, H. "Bacterial Lipopolysaccharides Structure, Synthesis, and Biological Activities"; American Chemical Society: Washington, DC, 1983; ACS Symp. Ser. No. 231, pp 121–140. Paulsen, H.; Hayauchi, Y.; Unger, F. M. *Carbohydr. Res.* **1983**, *111*, C5–C8.
(5) 2,3-Di-*O*-benzyl-D-mannose was prepared in six steps from commercially available methyl α-D-mannopyranoside ((a) isopropylmethyl ether, DMF, *p*-TsOH;[6] (b) BnBr, NaH, DMF; (c) AcOH 60%; (d) Ac_2O, pyridine; (e) Ac_2O, H_2SO_4; (f) MeONa, MeOH).
(6) Copeland, C.; Stick, R. V. *Aust. J. Chem.* **1978**, *31*, 1371–1374.
(7) Paquet, F.; Sinaÿ, P. *Tetrahedron Lett.* **1984**, 3071–3074. This phosphonate was used as a diastereoisomeric mixture.
(8) The *Z* geometry is deduced from the chemical shift of the vinylic proton of **11** ($CDCl_3$, 90 MHz) δ 6.26 (d, 1 H, J = 9 Hz). See: Ireland, R. E.; Mueller, R. H.; Willard, A. K. *J. Am. Chem. Soc.* **1976**, *98*, 2868–2877.

0002-7863/84/1506-8313$01.50/0 © 1984 American Chemical Society